



Supporting Information

for *Adv. Sci.*, DOI: 10.1002/advs.201800453

Subthreshold Operation of Organic Electrochemical Transistors for Biosignal Amplification

*Vishak Venkatraman, Jacob T. Friedlein, Alexander Giovannitti, Iuliana P. Maria, Iain McCulloch, Robert R. McLeod, and Jonathan Rivnay**

Supporting Information

Subthreshold operation of organic electrochemical transistors for bio-signal amplification

Vishak Venkatraman^{1,2}, Jacob T. Friedlein³, Alexander Giovannitti⁴,
Iuliana P. Maria⁴, Iain McCulloch^{4,5}, Robert R. McLeod³ and Jonathan
Rivnay^{1,2*}

Supporting Figures:

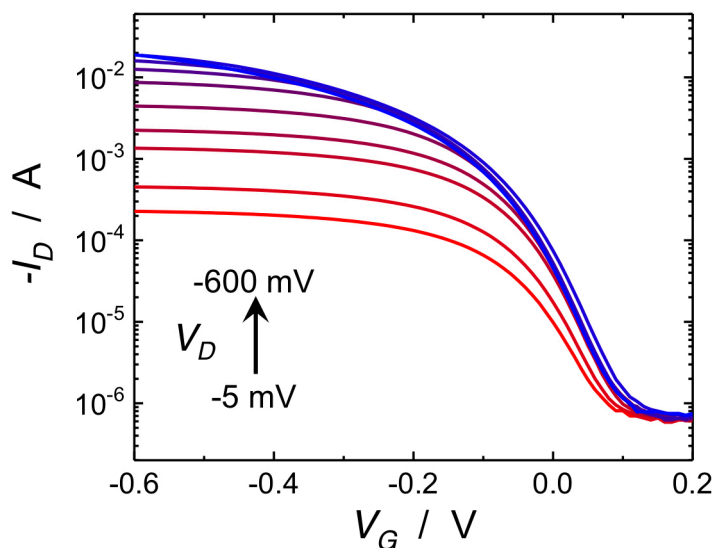


Figure S1. Transfer characteristics for $100 \mu\text{m} \times 10 \mu\text{m}$, 100 nm thick device at different drain voltages showing same subthreshold slope for a wide range of $-V_D$. (5, 10, 30, 50, 100, 200, 300, 400, 500, 600 mV)

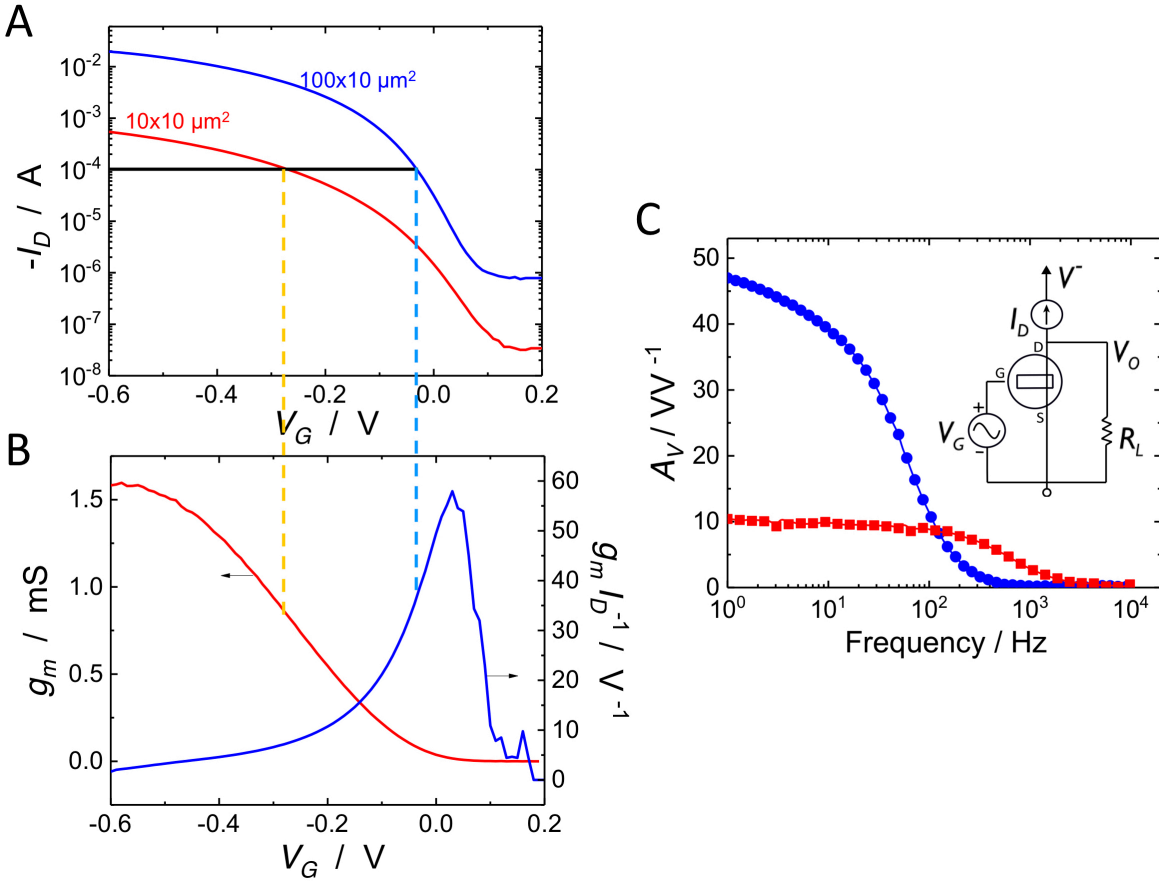


Figure S2. (A) Transfer curves of $100 \mu\text{m} \times 10 \mu\text{m}$ (200 nm thick) OEET, blue, and $10 \mu\text{m} \times 10 \mu\text{m}$ (50 nm thick) OEET, red. (B) Plots of transconductance, g_m , for the $10 \mu\text{m} \times 10 \mu\text{m}$ device, left axis, and g_m efficiency for the $100 \mu\text{m} \times 10 \mu\text{m}$ device. Solid black line denotes the constant operating current of $100 \mu\text{A}$, and resulting voltage and g_m (orange dashed line), and g_m efficiency values (blue dashed line) for each device in their intended operation regimes (superthreshold for the $10 \mu\text{m} \times 10 \mu\text{m}$ device, and subthreshold for the $100 \mu\text{m} \times 10 \mu\text{m}$ device). (C) Voltage gain as a function of frequency for the two devices; inset: circuit diagram of the setup used, where voltage gain, $A_V = \Delta V_o / \Delta V_G$

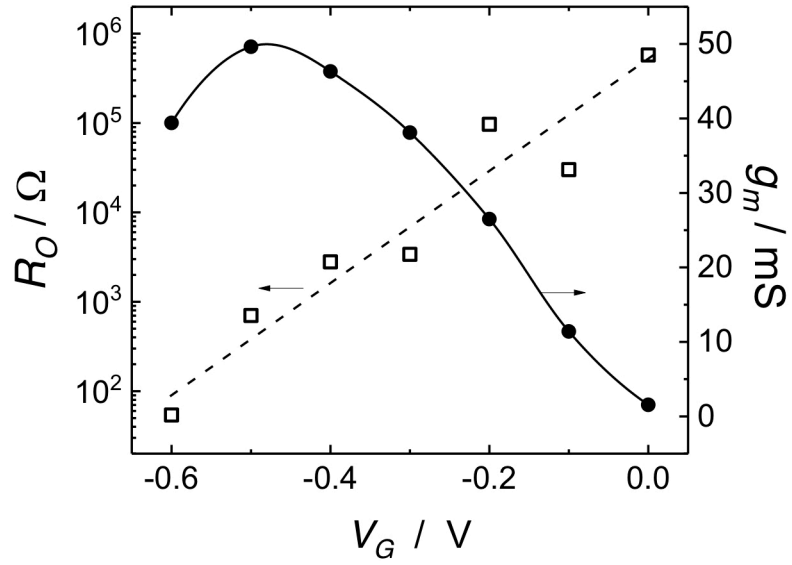


Figure S3. Output impedance, R_o , peak at different location than peak g_m , which affects the intrinsic voltage gain.

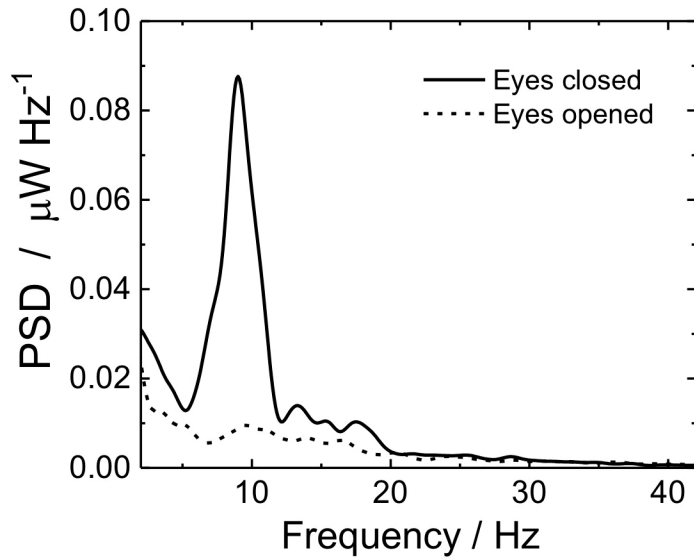


Figure S4. Power spectral density for EEG experiment in main text, for eye closed condition (observable 10 Hz alpha rhythms), and eyes opened.

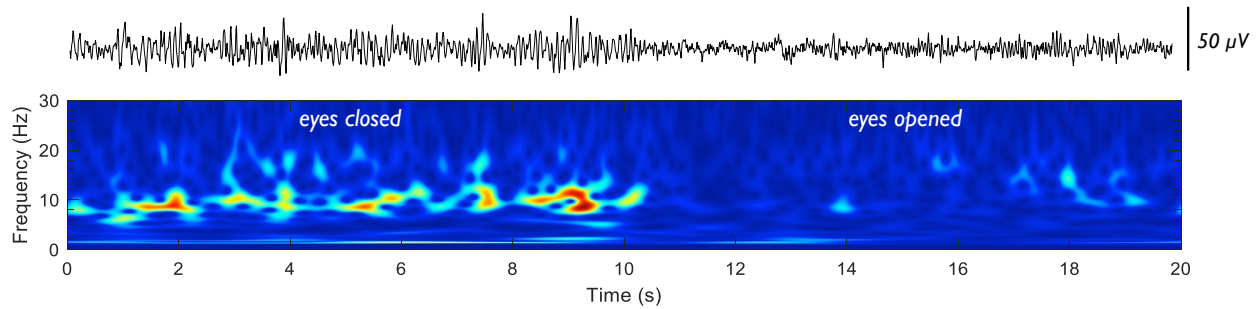


Figure S5. Time-frequency plot for EEG signals measured using 3M Red Dot adhesive medical electrodes recorded directly with the NI PXIe-4081 DMM, without the OECT or accompanying circuit. The periods of “eyes open” and “eyes closed” are noted for clarity. Note the voltage-time trace for the corresponding EEG signal of the DMM recording: the alpha wave amplitudes are $\sim 20\text{-}50\ \mu\text{V}$ peak-to-peak, as compared to the amplifier circuit, which measures the same signals at $\sim 1\text{-}2\ \text{mV}$.

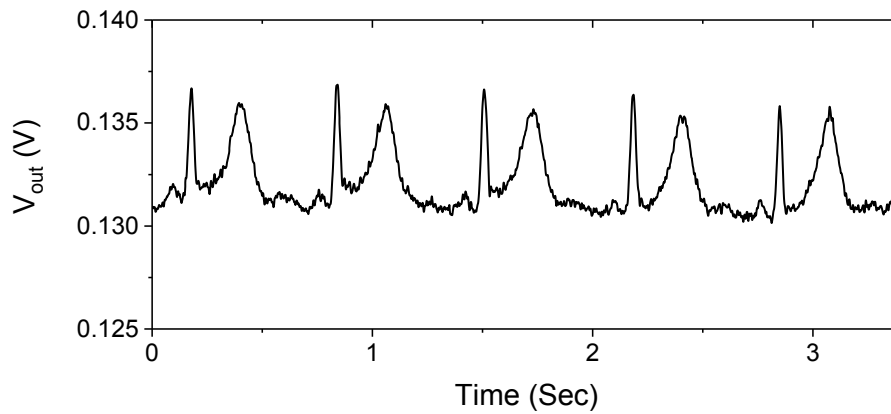


Figure S6. ECG signal recorded using OECT subthreshold amplifier circuit, using a feedback resistor of $19\ \text{k}\Omega$. The 3M Red Dot medical adhesive electrodes are attached on either side of the chest, and connected to the gate and source terminals of the OECT.

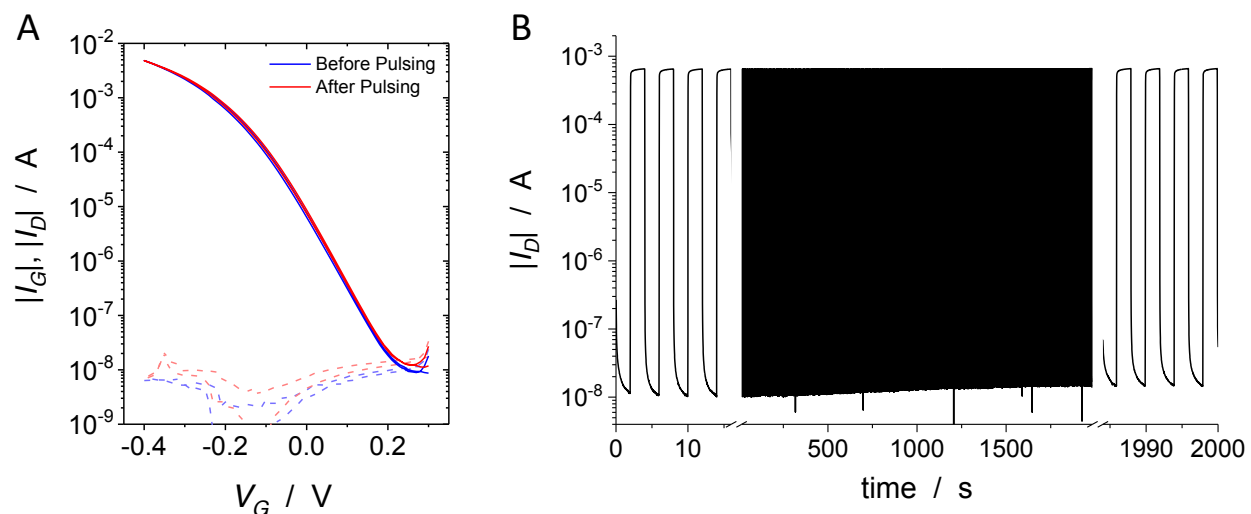


Figure S7. OECT stressing and threshold stability. A. Transfer characteristics (solid line: I_D , dashed line: I_G) before (blue) and after (red) continuous gate voltage pulsing for >30 minutes. $V_D = -0.4$ V. B. Drain current vs. time for the continuous pulsing experiment mentioned in (A). $V_D = -0.4$ V, with V_G pulsed between +0.3 V and -0.2 V, with a pulse duration of 2 s. This gate voltage range was selected to enable proper ranging of the current values without changing current range limits during acquisition with the NI PXIe SMUs. The observed shift in transfer characteristics after stressing is minimal, for example, I_D at $V_G = 0$ V increases from 7.7 μ A to 8.6 μ A (a shift of $\Delta V_G = -3.9$ mV) after 30 minutes of pulsed biasing.

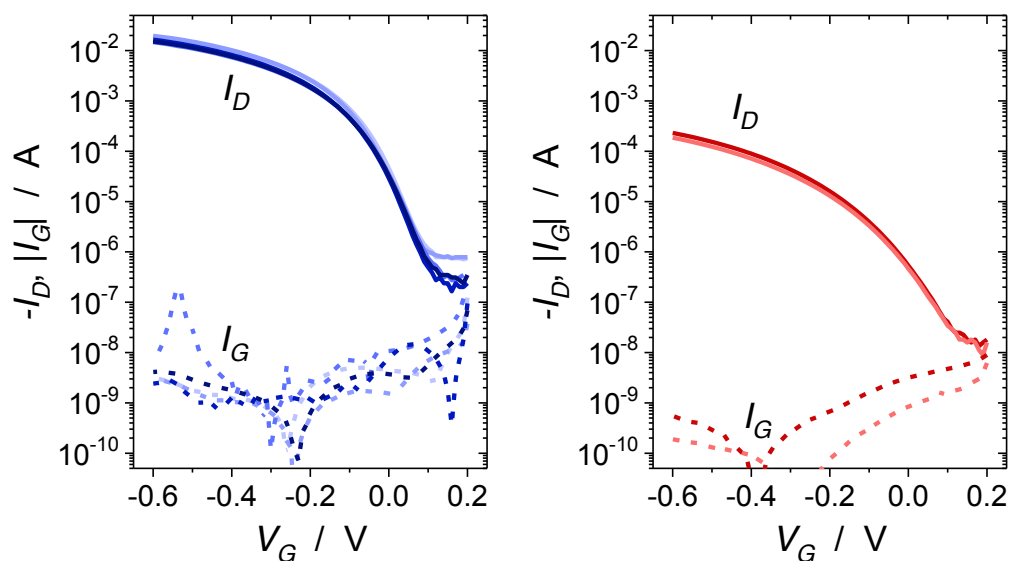


Figure S8. Transfer curves of 100 $\mu\text{m} \times 10 \mu\text{m}$ (200 nm thick) OEET, blue, and 10 $\mu\text{m} \times 10 \mu\text{m}$ (50 nm thick) OEET, red, devices showing both drain current (I_D , solid lines), and gate current (I_G ; dashed lines) for each device (different shading). Note that the drain current approaches the drain current in the transistor's "off" state.

Supporting Table:

Table S1. Fit results from data in Figure 4b, using the disorder model of main text reference 35.

<i>Material/device</i>	<i>DOS width (meV)</i>	<i>DOS peak position (meV)</i>	<i>Percolation fraction (%)</i>
p(g2T-TT) 10x10 μm^2	410 ± 60	-820 ± 290	0.1 ± 0.3
PEDOT:PSS 10x10 μm^2	811 ± 19	-254 ± 40	1.54 ± 0.4

Supporting method:

Comparing subthreshold and superthreshold regimes at the same current (I_D):

To achieve the same current for the two regimes of interest we use device geometry engineering: a $100\ \mu\text{m} \times 10\ \mu\text{m}$ ($W \times L$) transistor, 100 nm thick, shows subthreshold behavior at $I_D \sim 1\text{-}100\ \mu\text{A}$, while a $10\ \mu\text{m} \times 10\ \mu\text{m}$ transistor, 40 nm thick, is in its “superthreshold” region at $I_D = 100\text{-}500\ \mu\text{A}$ ($g_{m,\text{peak}} = 1.6\ \text{mS}$ at $V_G \sim 0.6\ \text{V}$). Fig S2a, shows the transfer characteristics of two devices of different dimensions. An operating point of $100\ \mu\text{A}$ is selected in order to be within the desired operation regime of both devices (superthreshold for the $10\ \mu\text{m} \times 10\ \mu\text{m}$ device, and subthreshold for the $100\ \mu\text{m} \times 10\ \mu\text{m}$ device). Fig S2b shows that while the resulting voltages due to $100\ \mu\text{A}$ operation are not exactly at the peak g_m , or peak g_m efficiency (or alternatively, peak SS), they are acceptably within the desired regime. More precise device engineering could result in a more ideal comparison, however, the present devices can be used as a proof of concept to make the comparisons of the two regimes.

In the above sample set, the $100\ \mu\text{m} \times 10\ \mu\text{m}$ device, operating at $100\ \mu\text{A}$ (subthreshold) has a transconductance value of $3.5\ \text{mS}$, while the $10\ \mu\text{m} \times 10\ \mu\text{m}$ device has a transconductance of $0.8\ \text{mS}$ at $100\ \mu\text{A}$. It can be inferred that in this comparison, keeping operating current at $100\ \mu\text{A}$, the subthreshold device’s higher g_m suggests a higher gain can be obtained – in line with the high transconductance efficiency discussed in the main text.

Since voltage output is often required for downstream signal processing, we explore voltage transduction by these devices using the circuit in Fig S2c, inset. A current source shunted with a load resistor (R_L) was used as the load and to set V_{DS} . The voltage gain in such a configuration can be calculated as $A_V = g_m \times R_L$. The load resistor R_L was chosen to be $20\ \text{k}\Omega$, to provide an A_V of 40 to 50 for the device operating at subthreshold. Care was taken to make sure the transistor was in saturation region by only applying a very small sinusoidal input of $1\ \text{mV}$. Similar to AC g_m analysis, the DC operating regions (Q point) of both

the devices, $100\ \mu\text{m} \times 10\ \mu\text{m}$ and $10\ \mu\text{m} \times 10\ \mu\text{m}$ p(g2T-TT), was biased at $100\ \mu\text{A}$ by choosing the appropriate V_G voltage. Figure S2c shows the results obtained. The subthreshold region of p(g2T-TT) $100\ \mu\text{m} \times 10\ \mu\text{m}$ outperformed (5 \times) the high g_m region of $10\ \mu\text{m} \times 10\ \mu\text{m}$ device with the same active material in terms of gain. However, the bandwidth was significantly lower, which can be expected due to high gain (constant gain bandwidth product theory).